

Passivity based Stability Assessment for Four types of Droops for DC Microgrids

Muhammad Anees
FREEDM System Center
North Carolina State University
Raleigh, USA
manees@ncsu.edu

Lisa Qi
ABB Corporate Research Center
ABB Inc.
Raleigh, USA
lisa.qi@us.abb.com

Mario Schweizer
ABB Corporate Research Center
ABB Inc.
Baden-Daettwil, Switzerland
mario.schweizer@ch.abb.com

Srdjan Lukic
FREEDM System Center
North Carolina State University
Raleigh, USA
smlukic@ncsu.edu

Abstract—DC microgrids are getting more and more applications due to simple converters, only voltage control and higher efficiencies compared to conventional AC grids. Droop control is a well know decentralized control strategy for power sharing among converter interfaced sources and loads in a DC microgrid. This work compares the stability assessment and control of four types of droops for boost converters using the concept of passivity. EN standard 50388-2 for railway systems provides a reference to ensure system stability in perspectives of converters and system integration. Low pass filter (LPF) in the feedback of the droop control is used to ensure converter passivity. Bus impedance is derived to ensure system passivity with less conservativeness. Analytical approach for design of passive controller for all four types of droops is verified through time domain simulations of a single boost converter based microgrid feeding a Constant Power Load (CPL).

Index Terms—DC Microgrids, Droop, Stability, Passivity

I. INTRODUCTION AND LITERATURE REVIEW

Different types of microgrids are based on the nature of electrical currents; AC, DC, or Hybrid microgrids. DC microgrid is considered simple and less complex than AC microgrids from a control perspective. Moreover, the inherent DC nature of renewables (PV and Wind etc.) and energy storage technologies (Batteries and fuel cells) makes DC microgrid a preferable choice from an integration perspective [1]. DC Microgrids are gaining more and more fame due to enhanced availability of the DC resources including energy generation (Photovoltaics and wind), storage (supercapacitors and batteries) and consumption (DC loads like HVAC, Lighting, DC fans etc.). Due to resources availability and improved efficiency in DC systems, DC microgrids have applications in diverse settings including data centers, off grid electrifications, telecommunications, electric vehicle charging stations, controlled indoor farming, maritime and offshore applications, military installations, commercial and residential buildings.

A. Hierarchical Control of DC Microgrids

Interconnection of the resources and loads in microgrids is possible through power electronics converters; regulation of the DC bus voltages through these converters is a primary control demand. The hierarchal control approach ensures the stable operation of microgrids, where each control layer is responsible for specific responsibilities based on the dynamic nature of responsibilities [2]. Hierarchal control for DC microgrids is given in Fig. 1. In Fig. 1, on the left, from bottom to top, are the control layers from device level to system level with objectives mentioned in the triangle. While on the right, from bottom to top, is the bandwidth of each control loop. Bandwidth of the lowest control loop is usually in microseconds – as a rule of thumb (6-10) times slower than the converter’s switching frequency. Examples of tracking control for converters are current control, voltage control and dual loop control [2]. As a rule of thumb, each outer control layer of the converter control is kept (6-10) times slower than the inner control layer. Following this hierarchy, outer voltage loop will be (6-10) times slower than the inner current loop and droop loop will be (6-10) times slower than outer voltage/current loop.

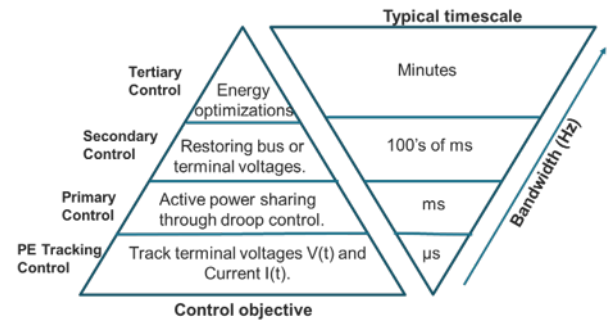


Fig. 1. Hierarchical Control of DC Microgrids

B. Droop Control

The idea of the droop control came from the AC generator, where the output power transfer from the generator is modulated with the frequency of operation. Following the same approach from the AC generator, droop control in converters of DC microgrids uses the terminal voltages of the converter as a signal for the intended power flow throughout the microgrid. There are multiple implementations of the droop reported in the literature [2-10]. From feedback variables perspective, droop can be categorized as power-based droop (VP and PV droop with droop coefficient k) and current based droop (IV and VI droop with droop coefficient d) [3]. There exists a fundamental conflict of uniform power sharing with voltage regulation because of non-uniform line impedances [5]. To resolve this conflict and improve the overall performance of the droop, different researchers proposed different methodologies [4-15]. Some of the approaches required communication and some don't. Communication enables the controllers for a coordinated action to regulate an average voltage and average power sharing correspondingly [5-7]. Decentralized approaches include the use of non-linear or adaptive droop gains [8-10]. Communication also enables the primary/droop controller to coordinate with the secondary controller using hierarchical control, which can use centralized or distributed control approach for the uniform power sharing along with the restoration/regulation of bus voltages [10-13].

C. Passivity based Droop Control Design

From a converter inner current control perspective, inductor current is controlled; in case of boost converter, inductor current is not same as output current. Therefore, for boost converter, both the inductor (input) and output current are measured. For a typical boost converter, all four types of droops can be represented by the following equations.

$$VI - \text{Droop} : v = v_o - d * i \quad (1)$$

$$VP - \text{Droop} : v = v_o - k * P \quad (2)$$

$$IV - \text{Droop} : i_0^* = \frac{v_o - v}{d}, i_L^* = (i_0^* - i_o) * G_{cc}(s) \quad (3)$$

$$PV - \text{Droop} : i_0^* = \frac{v_o - v}{k * v}, i_L^* = (i_0^* - i_o) * G_{cc}(s) \quad (4)$$

Voltage v in case of VI and VP droop will be fed to outer voltage loop of standard dual loop control. While reference current in case of IV and PV, will be fed to outer current loop that translate the output current to inductor current with $G_{cc}(s)$ as current controller in case of boost converter.

Knowing the structure of control loops, a small signal equivalent output impedance is deduced for four types of droops (IV, VI, PV, VP) for boost converter – sets of equations in Appendix I. The deduced equivalent small signal impedance has been verified through the time domain frequency sweeping simulations for each type of droop. Detailed derivation and verification through time domain simulation is not added to the paper due to pages limit but can be provided upon request.

Each of the above-mentioned droop type has their own advantages or disadvantages, but a detailed stability performance comparison of all four droops is still missing. At the same time passivity-based control design is currently a hot topic of research to ensure microgrid stability. Many papers have discussed DC system stability using passivity theorem either from converter design or system design perspectives [15-19]. Major contributions of this paper include 1) guidance for converter manufacturers and system integrators combining the European standard EN50388-2 and bus impedance passivity requirements [14] for stable DC microgrids, and 2) a comparison of performance (alternatively passivity characteristics) for four types of droops under varying microgrid conditions/parameters. Another important contribution is that Low pass filter bandwidth in primary droop control is used to make sure the both converter and system are passive, while the hierarchical control design remains intact.

II. CONVERTER AND SYSTEM PASSIVITY

Following the European standard EN50388-2 for AC traction system, the responsibility to maintain system stability is shared between the converter manufacturers and the infrastructure operator in an organizational tractable manner by the compliances with two rules [14]. Similarly, in DC systems, it is desirable to design the converter control and the overall system integration in such a way that we are ensuring the passivity of the converter and system.

- Equivalent converter impedances are strictly passive above a frequency threshold (87Hz in 16.6Hz railway; 300Hz in 50Hz applications).
“strictly passive” means that the complex converter impedance has positive real part for all frequencies above the threshold
- The grid is not allowed to have weakly-damped passive resonances below the frequency threshold, because converters are allowed to be non-passive there.

The above two requirements from EN50388-2 together guarantee system stability and can be used as converter and system design guideline without knowledge of the complete system, because parallel connected systems preserve passivity in the respective frequency range. Also, when more and more passive converters are added into the system which are passive with certain margin, the aggregated behavior of all converters is still passive. The concept to ensure converter passivity and system passivity for AC traction system stability can also be applied to DC microgrid stability. The frequency threshold of 300Hz may not be true in DC microgrid and can be derived from rigorous analysis.

The two requirements ensure system stability by 1) passive converters provided by converter manufacturers and 2) not allowing weakly-damped passive components in system integration by system integrators. The weakly-damped passive components in system integration is a conservative way to ensure system stability. Instead, bus impedance Z_{bus} offer an integrated way to ensure system passivity using the combination of all parallel impedances of the connected converters to

that bus [15]. For $m+n$ converters (m load converters, n source converters); equivalent bus impedance Z_{bus} can be computed as

$$Z_{bus} = Z_1 \parallel (Z_2 \parallel \dots \parallel Z_n) \parallel \dots \parallel (Z_{n+1} \parallel \dots \parallel Z_{m+n}) \quad (5)$$

For system stability, the equivalent Z_{bus} should follow the passivity criteria, which can be translated as: The *phase angle of Z_{bus} is between $\pm 90^\circ$ for the entire range to ensure passivity.*

TABLE I
SYSTEM PARAMETERS

Parameters	Value
Global no-load voltage ref [Vo]	350V
Source Voltages [E]	130V
Load Power	3600W
Source resistance [rBAT]	0.03Ω
Inductance [L]	2mH
Inductor ESR [r]	0.01Ω
Per meter line resistance [R]	10mΩ
Per meter line inductance [L]	10uH
Line length [LL]	29m
Bus Capacitance [C]	3.3mF
VI/IV droop coefficient [d]	1
VP/PV Droop coefficient [k]	10V/3600W
Current control bandwidth	3KHz
Voltage control bandwidth	200Hz
Outer current control bandwidth	200Hz
Switching frequency [fsw]	20KHz

Different researchers used different approaches for passivity-based converter controller design for DC microgrid [15-19]. Etc. Herein this paper, a conventionally used LPF implemented in the feedback of the droop control is used to make sure the converter is passive. There are different advantages of using LPF as a tweaking parameter to ensure system passivity. The most important one is that the tracking control (design of inner and outer loops) remains intact, while in other cases we need additional loops or filters that are directly impacting the other loops. Another important advantage is the emulation of virtual inertia in DC system through LPF BW selection – equivalent machine behavior using droop with LPF [20]. Using a simple microgrid of Fig. 2 as the test system, a boost converter powers a CPL through line impedance. Converter and microgrid passivity will be assessed using the specified parameters of Table 1. The converter's impedance plot displays non-passive regions around the current control loop bandwidth if no filter or LPF cutoff frequency is equal or above 50Hz despite classical control loop designs. Careful LPF bandwidth selection can ensure converter passivity. At the load input, a bus capacitance is present along with CPL. System analysis shows that even the converter becomes non-passive beyond a 50Hz bandwidth (Fig. 3), while the overall microgrid bus impedance remains passive. With bus impedance, even though there are some slight violations of passivity for converters, the system stability can still be ensured. This fact highlights the passivity

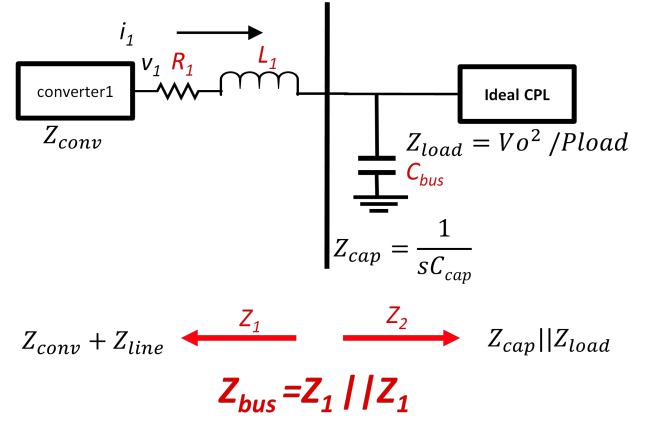


Fig. 2. Microgrid Model with CPL

of bus impedance to provide system stability while allowing some margins for converter design (Fig. 4).

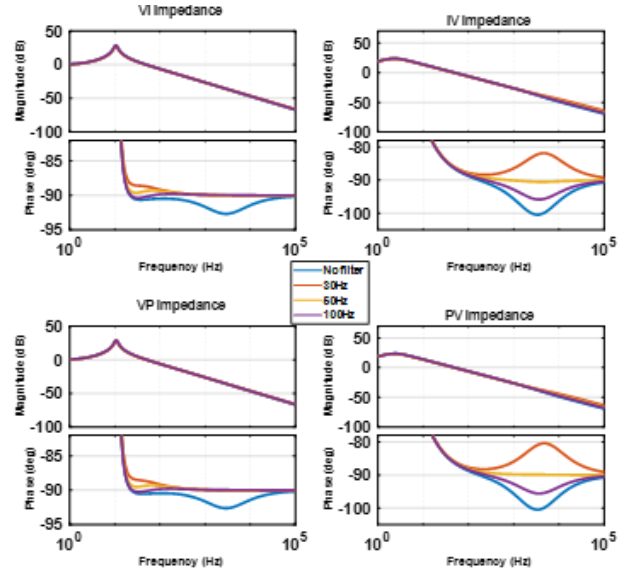


Fig. 3. Converter impedance around current loop BW

III. PARAMETERS IMPACTING MICROGRID PASSIVITY

There are different parameters which can impact the bus impedance, including the CPL power level, line impedance and bus capacitance. Now we will play with CPL power and line impedance to see its impact on bus impedance passivity. The bus capacitance case is ignored for this paper due to space constraint. Analytical findings are supported by time domain simulations, utilizing system parameters, unless otherwise noted.

A. Impact of CPL Power on System Passivity

Increasing the CPL power pushes the bus impedance to non-passive region, as observed in Fig. 5(a). At the standard rated power ($P=1x$), all four droops exhibit complete passivity with a 30Hz filter. However, when the CPL power increases to

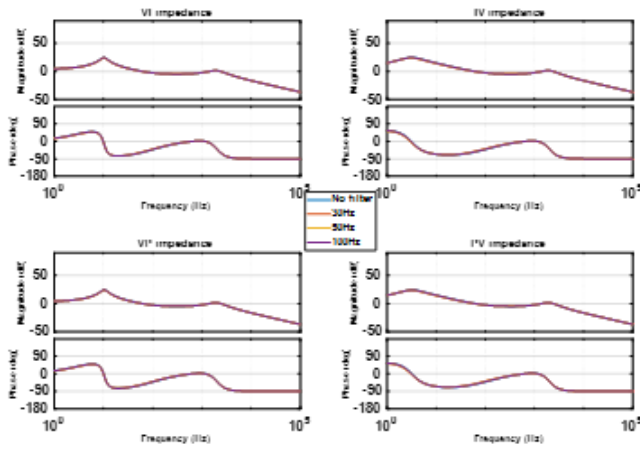


Fig. 4. Microgrid or bus impedance

3x (without LPF), all four droops show non-passive regions, necessitating at least a 30Hz LPF to eliminate the non-passive behavior. But the same 30Hz LPF doesn't suffice when the CPL power further escalates to 4x. In Fig. 5(b), time domain simulations reveal instability for all four droops at $P=4x$, with the 30Hz filter stabilizing oscillations at $P=3x$, as shown in the zoomed-in Fig. 5(c). These results delineate the CPL power's limit to destabilize the system from stable setpoints. Furthermore, the time domain simulations illustrate minor oscillations at $P=2x$ for IV and PV, but not for VI and VP. Consequently, for higher powers, VI and VP appear to be preferable choices compared to IV and PV.

B. Impact of Line Impedance on System Passivity

This case studies how line impedance impacts system passivity and the role of LPF in managing oscillations due to high inductive line impedance. With the line length increased to 10x and line inductance per meter set to 10uH at a $P=2x$ system operation level, Fig. 5(d) shows non-passive areas in the bus impedance for all four droop types at this increased line length. The corresponding time domain results in Fig. 5(e) reveal that the higher line impedance (without LPF) causes oscillations, aligning with non-passive zones from the analysis. A 100Hz filter controls these oscillations for IV and PV droops, while a 30Hz filter is needed for VI and VP. Zooming in (Fig. 5(f)) confirms that a 100Hz filter ensures full system passivity for IV and PV droops, not for VI and VP. For longer or more inductive lines, IV and PV droops are more suitable than VI and VP. The proposed approach in the article is verified on a single bus microgrid. The authors believe that this approach can be extended to multi-node and more complex DC microgrids as part of future research.

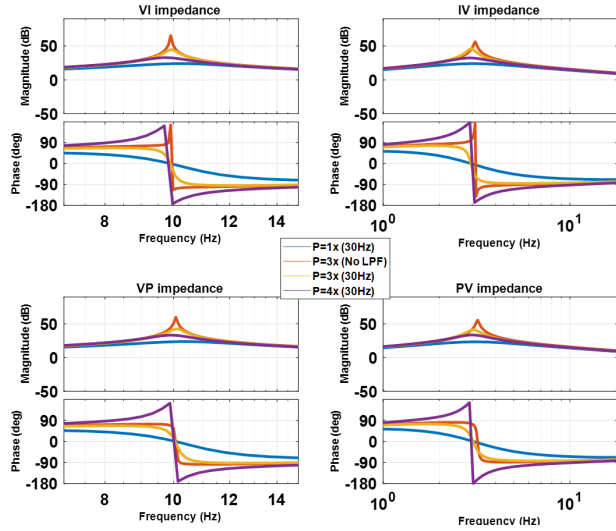
IV. CONCLUSION

This article provides a baseline approach for the assessment of system stability using passivity for droop-controlled DC microgrids. First, the passivity of the converter and microgrid is explained in the context of the EN standard 50388-2 for traction systems, the concept of bus impedance, and state of the art

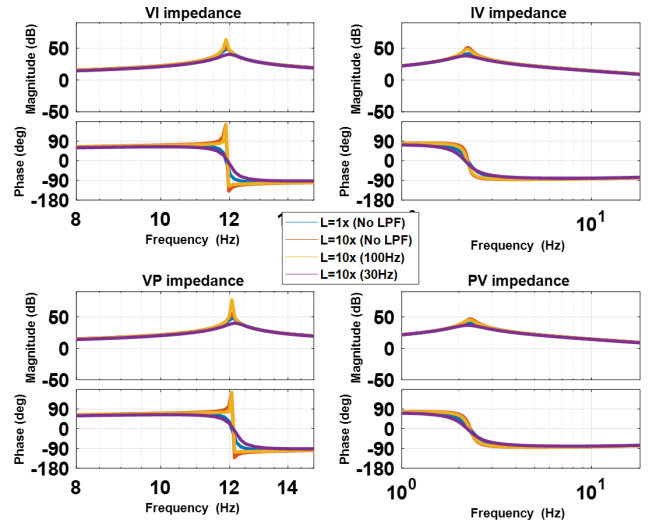
literature. Then a detailed approach for the assessment of the passivity of a converter/microgrid is provided. Conventional LPF is used to ensure the converter and microgrid passivity, which have major advantage of virtual inertia emulation and inner tracking control remains intact. Then a tweak for microgrid parameters is performed for four types of droops and it is found that for high power levels VI and VP is a preferable choice, IV and PV is a preferred choice for high line lengths and inductances.

REFERENCES

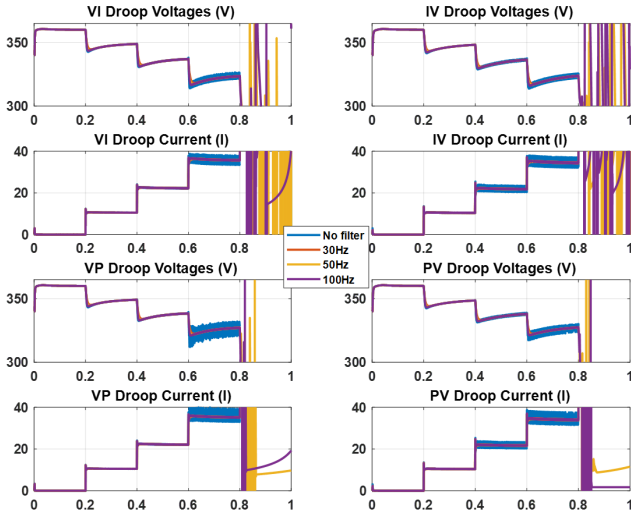
- [1] L. Xu and D. Chen, "Control and Operation of a DC Microgrid With Variable Generation and Energy Storage," in *IEEE Transactions on Power Delivery*, vol. 26, no. 4, pp. 2513-2522, Oct. 2011, doi: 10.1109/TPWRD.2011.2158456.
- [2] J. M. Guerrero, J. C. Vasquez, J. Matas, L. G. de Vicuna and M. Castilla, "Hierarchical Control of Droop-Controlled AC and DC Microgrids—A General Approach Toward Standardization," in *IEEE Transactions on Industrial Electronics*, vol. 58, no. 1, pp. 158-172, Jan. 2011, doi: 10.1109/TIE.2010.2066534.
- [3] F. Gao, R. Kang, J. Cao and T. Yang, "Primary and secondary control in DC microgrids: a review," in *Journal of Modern Power Systems and Clean Energy*, vol. 7, no. 2, pp. 227-242, March 2019, doi: 10.1007/s40565-018-0466-5.
- [4] T. Dragičević, X. Lu, J. C. Vasquez and J. M. Guerrero, "DC Microgrids—Part I: A Review of Control Strategies and Stabilization Techniques," in *IEEE Transactions on Power Electronics*, vol. 31, no. 7, pp. 4876-4891, July 2016, doi: 10.1109/TPEL.2015.2478859.
- [5] X. Lu, J. M. Guerrero, K. Sun and J. C. Vasquez, "An Improved Droop Control Method for DC Microgrids Based on Low Bandwidth Communication With DC Bus Voltage Restoration and Enhanced Current Sharing Accuracy," in *IEEE Transactions on Power Electronics*, vol. 29, no. 4, pp. 1800-1812, April 2014, doi: 10.1109/TPEL.2013.2266419.
- [6] M. Mokhtar, M. I. Marei and A. A. El-Sattar, "An Adaptive Droop Control Scheme for DC Microgrids Integrating Sliding Mode Voltage and Current Controlled Boost Converters," in *IEEE Transactions on Smart Grid*, vol. 10, no. 2, pp. 1685-1693, March 2019, doi: 10.1109/TSG.2017.2776281.
- [7] F. Li, Z. Lin, Z. Qian and J. Wu, "Active DC bus signaling control method for coordinating multiple energy storage devices in DC microgrid," 2017 IEEE Second International Conference on DC Microgrids (ICDCM), Nuremberg, Germany, 2017, pp. 221-226, doi: 10.1109/ICDCM.2017.8001048.
- [8] P. Prabhakaran, Y. Goyal and V. Agarwal, "Novel Nonlinear Droop Control Techniques to Overcome the Load Sharing and Voltage Regulation Issues in DC Microgrid," in *IEEE Transactions on Power Electronics*, vol. 33, no. 5, pp. 4477-4487, May 2018, doi: 10.1109/TPEL.2017.2723045.
- [9] J. Su, K. Li, Y. Li, C. Xing and J. Yu, "A Novel State-of-Charge-Based Droop Control for Battery Energy Storage Systems to Support Coordinated Operation of DC Microgrids," in *IEEE Journal of Emerging and Selected Topics in Power Electronics*, vol. 11, no. 1, pp. 312-324, Feb. 2023, doi: 10.1109/JESTPE.2022.3149398.
- [10] J. Ni, B. Zhao, A. Goudarzi, Y. Li and J. Xiang, "A Dispatchable Droop Control Method for PV Systems in DC Microgrids," in *IEEE Access*, vol. 11, pp. 7588-7598, 2023, doi: 10.1109/ACCESS.2023.3237591.
- [11] T. Dragicevic, J. M. Guerrero, J. C. Vasquez, D. Skrlec, "Supervisory Control of an Adaptive-droop Regulated DC Microgrid With Battery Management Capability," in *IEEE Trans. On Power Electronics*, Vol. 29, No. 2, Feb 2014.
- [12] J. Su, K. Li, L. Zhang, X. Pan and J. Yu, "A Decentralized Power Allocation Strategy for Dynamically Forming Multiple Hybrid Energy Storage Systems Aided With Power Buffer," in *IEEE Transactions on Sustainable Energy*, vol. 14, no. 3, pp. 1714-1724, July 2023, doi: 10.1109/TSTE.2023.3244335.
- [13] C. Jin, P. Wang, J. Xiao, Y. Tang and F. H. Choo, "Implementation of Hierarchical Control in DC Microgrids," in *IEEE Transactions on Industrial Electronics*, vol. 61, no. 8, pp. 4032-4042, Aug. 2014, doi: 10.1109/TIE.2013.2286563.



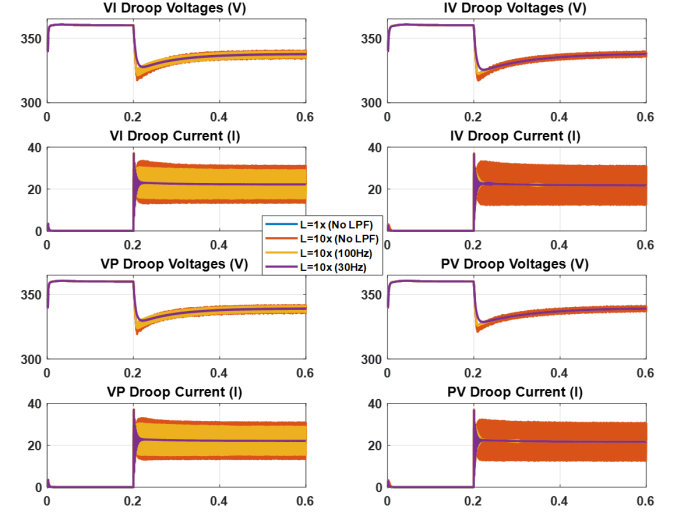
(a) Analytical results for increasing CPL power



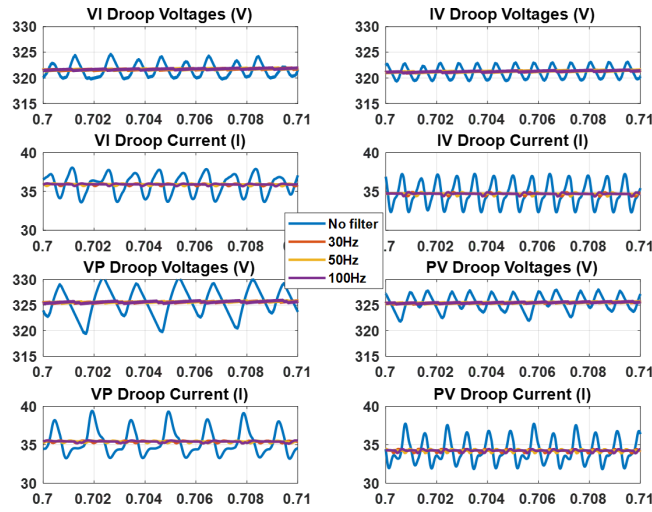
(d) Analytical results for increasing line length



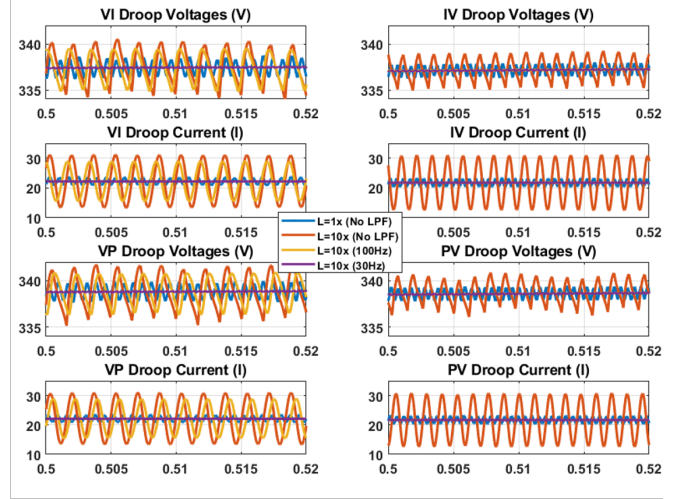
(b) Time domain results for increasing CPL power



(e) Time domain results for increasing line length



(c) Time domain results – zoomed in



(f) Time domain results – zoomed in

Fig. 5. Effect of CPL power and line impedance on microgrid passivity

- [14] CLC PREN 50388 -2, "Railway Applications - Fixed installations and rolling stock - Technical criteria for the coordination between power supply and rolling stock to achieve interoperability - Part 2: stability and harmonics" . [Online]. Available: <https://standards.iteh.ai/catalog/standards/clc/f5fb00d6-1f29-4dd4-a8fd-e3e478907499/pren-50388-2-2017>. [Accessed sept ,3 ,2023]
- [15] Y. -C. Jeung, D. -C. Lee, T. Dragičević and F. Blaabjerg, "Design of Passivity-Based Damping Controller for Suppressing Power Oscillations in DC Microgrids," in IEEE Transactions on Power Electronics, vol. 36, no. 4, pp. 4016-4028, April 2021, doi: 10.1109/TPEL.2020.3024716.
- [16] M. Afkar, R. Gavagsaz-Ghoachani, M. Phattanasak and S. Pierfederici, "Decentralized Passivity-based control of two distributed generation units in DC microgrids," 2023 8th International Conference on Technology and Energy Management (ICTEM), Mazandaran, Babol, Iran, Islamic Republic of, 2023, pp. 1-5, doi: 10.1109/ICTEM56862.2023.10084246.
- [17] L. Eggenschwiler, P. Favre-Perrod, M. Adly and K. Strunz, "Closed-loop impedance calculation of grid-tied three-phase inverters/rectifiers in bus signaling strategy-controlled DC microgrids," 2017 IEEE Second International Conference on DC Microgrids (ICDCM), Nuremberg, Germany, 2017, pp. 309-315, doi: 10.1109/ICDCM.2017.8001062.
- [18] Z. Wang, J. Wang and M. Zhang, "An Adaptive Nonlinear Control Strategy for DC-DC Converter with Constant Power Load Based on Passivity-Based Control," 2021 IEEE Sustainable Power and Energy Conference (iSPEC), Nanjing, China, 2021, pp. 2869-2874, doi: 10.1109/iSPEC53008.2021.9735967.
- [19] J. S. Velez, S. Ospina and E. Giraldo, "Passivity-Based Control for a Buck-Boost Converter Applied in Small Wind Generation Interconnected to DC Microgrid," 2019 IEEE 4th Colombian Conference on Automatic Control (CCAC), Medellin, Colombia, 2019, pp. 1-6, doi: 10.1109/CCAC.2019.8920939.
- [20] H. Tu, H. Yu and S. Lukic, "Impact of Virtual Inertia on DC Grid Stability With Constant Power Loads," in IEEE Transactions on Power Electronics, vol. 38, no. 5, pp. 5693-5699, May 2023, doi: 10.1109/TPEL.2023.324313.

APPENDIX I

Notation followed from Table 1, where,

$$Z(s) = r_{\text{BAT}} + r_f + Ls, d = R_{\text{vd}}, k_{pv} = k_{vp} = k, \\ Dc = \text{duty cycle}$$

$$Z^{\text{PV}} = \frac{((1-Dc) + I_L G_c(s)) V_{\text{BUS}} G_c(s) G_{cc}(s) + (1 - I_L G_c(s) G_{cc}(s)) (Z(s) + V_{\text{BUS}} G_c(s))}{[(1-Dc) + I_L G_c(s)] [(1-Dc) + (V_{\text{BUS}} G_c(s) G_{cc}(s) V_{\text{ref}}) / (k_{pv} V_{\text{BUS}}^2)] + [Z(s) + V_{\text{BUS}} G_c(s)] (sC - (I_L G_c(s) G_{cc}(s) V_{\text{ref}}) / (k_{pv} V_{\text{BUS}}^2))}$$

$$Z^{\text{IV}} = \frac{((1-Dc) + I_L G_c(s)) V_{\text{BUS}} G_c(s) G_{cc}(s) + (1 - I_L G_c(s)) (Z(s) + V_{\text{BUS}} G_c(s))}{[(1-Dc) + I_L G_c(s)] [(1-Dc) + (V_{\text{BUS}} G_c(s) G_{cc}(s)) / R_{\text{vd}}] + [Z(s) + V_{\text{BUS}} G_c(s)] (sC - (I_L G_c(s) G_{cc}(s)) / R_{\text{vd}})}$$

$$Z^{\text{VI}} = \frac{[(1-Dc) V_{\text{BUS}} - I_L Z(s)] R_{\text{vd}} G_c(s) G_v(s) + V_{\text{BUS}} G_c(s) + Z(s)}{[(1-Dc) V_{\text{BUS}} - I_L Z(s)] G_c(s) G_v(s) + [V_{\text{BUS}} G_c(s) + Z(s)] sC + (1-Dc) I_L G_c(s) + (1-Dc)^2}$$

$$Z^{\text{VP}} = \frac{[(1-Dc) k_{vp} V_{\text{BUS}}^2 - I_L Z(s) k_{vp} V_{\text{BUS}}] G_c(s) G_v(s) + V_{\text{BUS}} G_c(s) + Z(s)}{[(1-Dc) V_{\text{ref}} - V_{\text{ref}} / V_{\text{BUS}} I_L Z(s)] G_c(s) G_v(s) + [sC V_{\text{BUS}} + (1-Dc) I_L] G_c(s) + sC Z(s) + (1-Dc)^2}$$